Chemical Engineering Journal 94 (2003) 19–28

Chemical Engineering Journal

www.elsevier.com/locate/cej

Relationship between the kinetic parameters of different catalyst deactivation models

A. Monzón [a,*], E. Romeo [a], A. Borgna [b]

[a] Department of Chemical and Environmental Engineering, Faculty of Science, University of Zaragoza 50009, Zaragoza, Spain
[b] INCAPE (FIQ-UNL-CONICET), Santiago del Estero 2654, 3000, Santa Fe, Argentina

Received 1 March 2002; accepted 12 December 2002

Abstract

This paper presents a mathematical relationship between the parameters of *Levenspiel's Deactivation Kinetic Model* (*LDKM*) and those of the *Deactivation Models with Residual Activity* (*DMRA*) and their evolution over time. This correlation provides an explanation for the erroneous variation obtained in the kinetic parameters (*deactivation order and deactivation function*) over time when *LDKM* is used to fit deactivation data having a certain level of residual activity, which frequently leads to systematic errors in estimating intrinsic parameters, such as activation energies. The variations of the *LDKM* parameters cannot in fact be related to a physical phenomenon, but are only a consequence of a mathematical artifact. The methodology developed in this work provides a valuable tool for the comparison and discrimination between different models used in kinetic studies. The equations here presented are applied to analyze the deactivation by fouling of Pt/Al_2O_3 reforming catalysts during methyl cyclohexane dehydrogenation.

Keywords: Deactivation kinetic models; Residual activity; Variable deactivation order; Parameter estimation; Pt/Al_2O_3; Catalytic reforming; Fouling; Methyl-cyclohexane dehydrogenation

---

1. Introduction

One of the main problems in the estimation and interpretation of kinetic parameters lies in the choice of the most suitable kinetic model. An inappropriate choice of kinetic model can result in misleading conclusions about the mechanism involved in the reaction under consideration [1].

In this context, the *Deactivation Kinetic Model* proposed by Szepe and Levenspiel, *LDKM*, [2], has been widely used in the area of the kinetics of catalyst deactivation to calculate the loss of catalytic activity, a, over reaction time.

$$-\frac{\mathrm{d}a}{\mathrm{d}t} = \psi_d(p_i, T)a^d \tag{1}$$

The two kinetic parameters appearing in this model are called "*deactivation function*", ψ_d, and "*deactivation order*", d, respectively. The deactivation order depends on the mechanism involved in the deactivation process and, in principle, d must be constant throughout the reaction. The deactivation function takes into account the influence on the deactivation rate of the operating conditions, i.e. reaction temperature and concentration of reactants, products and poisons. The explicit form of the deactivation function can be of the pseudo-homogeneous type [2,3].

$$-\frac{\mathrm{d}a}{\mathrm{d}t} = (k_d p_\mathrm{A}^m)a^d \tag{2a}$$

or of the *LHHW* type, usually deduced from mechanistic developments [4–9].

$$-\frac{\mathrm{d}a}{\mathrm{d}t} = \left(\frac{k_d p_\mathrm{A}^m}{(1+\sum K_i p_i)^m}\right)a^d \tag{2b}$$

This equation is usually used in its integrated form. Thus, if the kinetic parameters d and ψ_d can be considered as constants, the integration of Eq. (1) leads to the following expressions:

$$a = \exp(-\psi_d t); \quad d = 1 \tag{3a}$$

$$a = \frac{1}{(1+(d-1)\psi_d t)^{1/(d-1)}}; \quad d \neq 1 \tag{3b}$$

The *LDKM* represented a significant advance in the development of the kinetic modeling of catalyst deactivation, since it was demonstrated that the majority of the empirical kinetic models previously proposed were particular cases of

---

[*] Corresponding author. Present address: Departmento de Ingenieria Quimica y Tecnologias del Medio Ambiente, University of Zaragoza, Zaragoza 50009, Spain. Tel.: +34-976-761157; fax: +34-976-762142.
E-mail address: amonzon@posta.unizar.es (A. Monzón).

1385-8947/03/$ – see front matter © 2003 Elsevier Science B.V. All rights reserved.
doi:10.1016/S1385-8947(03)00002-0

the *LDKM* [2]. In spite of this, the *LDKM* is not a sufficiently general model, one of its limitations being that it predicts that the catalyst activity always falls to zero [10,11]. Thus, if the value of the deactivation order is greater or equal to 1, the catalyst takes an infinite time to deactivate completely. If the value of d is ranged between zero and one, then the *LDKM* predicts a total deactivation of the catalyst over a finite time [12].

However, it is frequently found that the catalyst is not completely deactivated but reaches a residual activity level clearly distinct from zero [10,11,13–26]. This residual activity is a function of the operating conditions and of the nature of the catalyst. Among other reasons, the appearance of a residual activity has been attributed to the presence of a reversible deactivation process [13,15,18–21], or to the presence of a fraction of the active sites of the catalyst that are not deactivated [11,13,27]. For instance, the existence of a residual dispersion has frequently been observed during catalyst sintering [22–26]. When the catalysts exhibit residual activity, more general models to predict the presence of this residual activity should be used. These models are called *General Power Law Equations*, *GPLE*, [10], or *Deactivation Models with Residual Activity*, *DMRA*, [11]. Several examples of these models are presented further

$$-\frac{\mathrm{d}a}{\mathrm{d}t} = \psi_d^*(p_i, T)a^{d^*} - \psi_\mathrm{S}(p_i, T) \tag{4a}$$

$$-\frac{\mathrm{d}a}{\mathrm{d}t} = \psi_d^*(p_i, T)a^{d^*} - \psi_\mathrm{S}(p_i, T)a^{d_\mathrm{S}} \tag{4b}$$

$$-\frac{\mathrm{d}a}{\mathrm{d}t} = \psi_d^*(p_i, T)(a - a_\mathrm{S}(p_i, T))^{d^*} \tag{4c}$$

$$-\frac{\mathrm{d}a}{\mathrm{d}t} = \psi_d^*(p_i, T)a^{d^*} + \psi_\mathrm{S}(p_i, T)a - \psi_\mathrm{S}(p_i, T)a^{d_\mathrm{S}} \tag{4d}$$

The above equations are different generalizations of the *LDKM* and in each case the value of the residual activity, a_S, is calculated as the root of the equation $\mathrm{d}a/\mathrm{d}t = 0$.

When analyzing activity-time data showing a given value of residual activity, it is better to use some of the *DMRA* expressions in the equations above in order to obtain reliable kinetic parameters. On the other hand, if the *LDKM* is used, it is found that both the deactivation order and the deactivation function vary over the reaction time [10,26–29]. It has frequently, been postulated that a variation of the deactivation order is a consequence of a change in the deactivation mechanism [27–29] or due to the influence of diffusional effects in the reaction kinetics [30]. However, as has already been pointed out [10,11,26], such variations in the parameters do not usually have a physical basis and are only a consequence of using an inadequate model. Another consequence related to the use of the *LDKM* is that the values of the intrinsic kinetic parameters of Eq. (2a and b) (activation energies, pre-exponential factors, kinetic reaction orders and constants of adsorption) are usually overestimated [26].

In spite of the above, no mathematical explanation has been suggested for the variation in the deactivation order when the *LDKM* is used to fit deactivation data with residual activity. Thus, as far as we know, a mathematical relationship between the *LDKM* and *DMRA* parameters and their evolution over time has not been proposed. In this work, we present a methodology that allows the correlation of the parameters of different deactivation kinetic models and their evolution as a function of time. The aim of this work is not to propose new methods for fitting kinetic data, but rather to emphasize the importance of using appropriate models to reach conclusions with a real physical meaning [10,26].

Finally, these equations have been applied to analyze the deactivation by fouling of a reforming $\mathrm{Pt/Al_2O_3}$ catalyst during the dehydrogenation of methyl cyclohexane [31,32].

2. Relationship between the kinetic parameters of *LDKM* and *DMRA*

In this section, a relationship between the intrinsic parameters of the *LDKM* and *DMRA* is established. Eq. (4c) is used here for representing the *DMRA* because it is the most frequently found in the literature [10,11,22–26]. However, it should be emphasized that similar correlations can also be obtained for other *DMRA* equations.

When Eq. (4c) is used to analyze experimental data, it is usually found that the deactivation order, d^*, is 1 or 2 [10,22–26]. In these cases, the following expressions for the deactivation rate and activity evolution are obtained.

For $d^* = 1$

$$-\frac{\mathrm{d}a}{\mathrm{d}t} = -a' = \psi_{d_1}^*(a - a_{\mathrm{S}_1}) \tag{5}$$

$$a = a_{\mathrm{S}_1} + (1 - a_{\mathrm{S}_1})\exp(-\psi_{d_1}^* t) \tag{6}$$

and for $d^* = 2$

$$-\frac{\mathrm{d}a}{\mathrm{d}t} = -a' = \psi_{d_2}^*(a - a_{\mathrm{S}_2})^2 \tag{7}$$

$$a = a_{\mathrm{S}_2} + \frac{(1 - a_{\mathrm{S}_2})}{1 + (1 - a_{\mathrm{S}_2})\psi_{d_2}^* t} \tag{8}$$

Given that in Eqs. (5) and (7) the value of d^* has been fixed, these models have two parameters which can be fitted, $\psi_{d_i}^*$ and a_{S_i}, as in the case of the model described by the *LDKM* (Eq. (1)), for which the fitting parameters are ψ_d and d.

At this point, the goal is to predict the values that the parameters of *LDKM*, (ψ_d and d), should have in order to be able to fit a set of experimental data showing residual activity, following the same pattern as that described by the *DMRA* (Eqs. (6) or (8)). *LDKM* and *DMRA* should therefore predict the same activity values as a function of time. Assuming that the deactivation rate predicted for both models, *LDKM* and *DMRA* is the same, it is obtained that

$$(-a') = \psi_d a^d = \psi_{d_2}^*(a - a_{\mathrm{S}_2})^2 \tag{9}$$

From the above expression, explicit equations for d and ψ_d of the following type can be obtained:

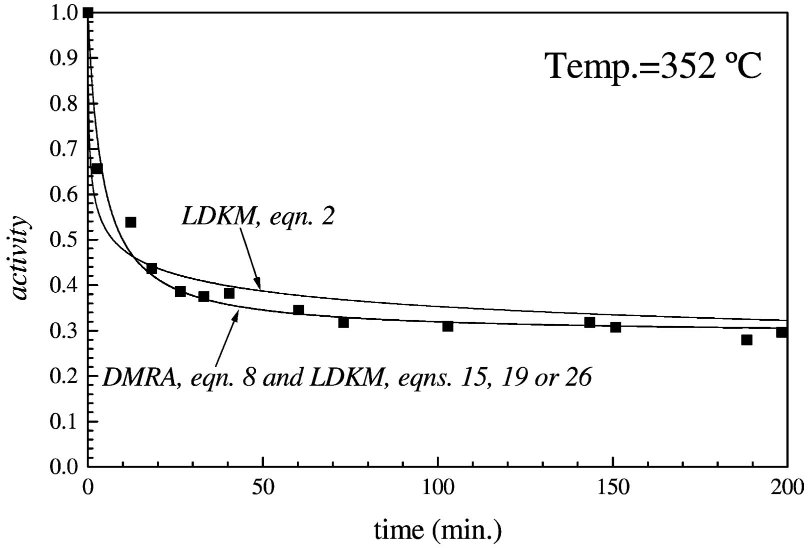

Fig. 1. Fit of the experimental data at 352 °C, obtained from Jossens and Petersen [31]. Comparison of different deactivation kinetic models.

$$d=\varphi_1(\psi_d, a_S, \psi_d^*, t) \tag{10}$$

$$\psi_d=\varphi_2(d, a_S, \psi_d^*, t) \tag{11}$$

Using Eqs. (10) and (11), an infinite number of sets of pairs $\{d,\ \psi_d\}$ allows the calculation of identical activity–time curves as predicted by the *DMRA*. It should be emphasized that at least one, or both, of these parameters must vary over time. In the simplest cases, we can assume that one of these parameters is constant and consequently the other can be obtained as a function of time. Three cases have been developed for obtaining sets of pairs $\{d,\ \psi_d\}$ which allow for the simulation of the a_{DMRA} curves. In the first case the *deactivation order* is maintained constant and the variation in the *deactivation function*, ψ_d is calculated. The second case is the opposite, i.e. d is variable and ψ_d is constant, and in the third case both parameters are varied.

Case 1 (d variable, ψ_d constant). From Eq. (1), the *deactivation order* as a function of time can be obtained as follows:

$$d(t)=\ln\frac{(-a'/\psi_d)}{\ln(a)} \tag{12}$$

In the above equation, both a' and a can be computed by using any of the *DMRA* equations. In the present case, Eqs. (7) and (8) have been used. By substituting Eqs. (7) and (8) in Eq. (12), the deactivation order d as a function of time can be obtained as follows:

$$d(t)=\frac{\ln(\psi_{d_2}^*(a_{\mathrm{DMRA}}-a_{S_2})^2/\psi_d)}{\ln(a_{\mathrm{DMRA}})} \tag{13}$$

$$d(t)=\ln\left(\frac{\psi_{d_2}^*}{\psi_d}\left(\frac{1-a_{S_2}}{1+(1-a_{S_2})\psi_{d_2}^* t}\right)^2\right)\times\left(\ln\left(a_{S_2}+\frac{1-a_{S_2}}{1+(1-a_{S_2})\psi_{d_2}^* t}\right)\right)^{-1} \tag{14}$$

Eq. (14) leads to the evolution of d as a function of time for a given set of fixed values of the parameters ψ_d, $\psi_{d_2}^*$ and a_{S_2}. Using these $d(t)$ data, the activity decay can be computed solving the following differential equation:

$$\frac{\mathrm{d}a}{\mathrm{d}t}=-\psi_d a^{d(t)} \tag{15}$$

As was expected, the activity values predicted by Eqs. (15) and (8) are equal as a consequence of Eq. (9), Figs. 1–3.

Case 2 (ψ_d variable, d constant). As in the Case 1, the evolution of the *deactivation function* with time can be obtained from Eq. (1).

$$\psi_d(t)=\frac{a'}{a^d} \tag{16}$$

Thus, substituting Eqs. (7) and (8) in Eq. (16) leads to

$$\psi_d(t)=\frac{\psi_{d_2}^*(a_{\mathrm{DMRA}}-a_{S_2})^2}{a_{\mathrm{DMRA}}^d} \tag{17}$$

$$\psi_d(t)=\psi_{d_2}^*\left(\frac{1-a_{S_2}}{1+(1-a_{S_2})\psi_{d_2}^* t}\right)^2\times\left(a_{S_2}+\frac{1-a_{S_2}}{1+(1-a_{S_2})\psi_{d_2}^* t}\right)^{-d} \tag{18}$$

Eq. (18) leads to the evolution of ψ_d as a function of time for a given set of fixed values of the parameters d, $\psi_{d_2}^*$ and a_{S_2}. Using again these $\psi_d(t)$ data, the activity can be calculated again solving the differential Eq. (1).

$$\frac{\mathrm{d}a}{\mathrm{d}t}=-\psi_d(t)a^d \tag{19}$$

Again, the activity values predicted by Eqs. (19) and (8) are equal, Figs. 1–3. It is important to note that both cases presented here are equivalent in that they both predict the same value of catalyst activity.

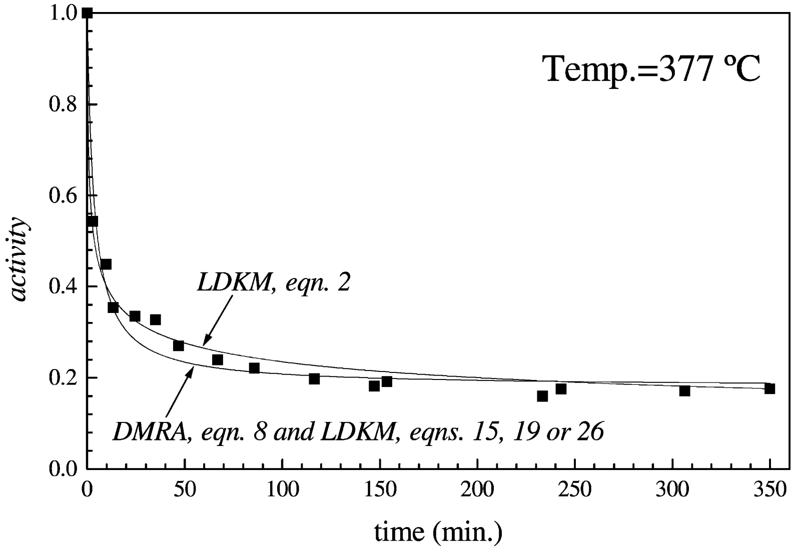

Fig. 2. Fit of the experimental data at 377 °C, obtained from Jossens and Petersen [31]. Comparison of different deactivation kinetic models.

Case 3 (ψ_d and d variables). In this case both parameters vary. Now, the main difficulty is to determine previously the variation of one of the parameters, and then to calculate the other. Frequently, the calculation of the *deactivation order of LDKM* is made using the slope of the $\log(a)$ versus $\log(t)$ plot. The equation corresponding to this plot is

$$a = At^m \Leftrightarrow \ln(a) = \ln(A) + m\ln(t) \tag{20}$$

This equation is an approximation of the Eq. (3b), for the case in which $(d-1)\psi_d t \gg 1$, [2]

$$a \cong ((d-1)\psi_d t)^{1/(1-d)} \tag{21}$$

and therefore

$$\ln(a) \cong \frac{1}{1-d}\ln((d-1)\psi_d t) = \frac{\ln((d-1)\psi_d)}{(1-d)} + \frac{1}{1-d}\ln(t) \tag{22}$$

From the above equation it can be seen that the exponent m can be experimentally calculated as

$$m = \frac{1}{1-d} = \frac{d(\ln(a))}{d(\ln(t))} = \frac{(a')t}{a} \tag{23}$$

It is frequently observed that the deactivation data displayed in a $\log(a)$ versus $\log(t)$ plot do not show a linear

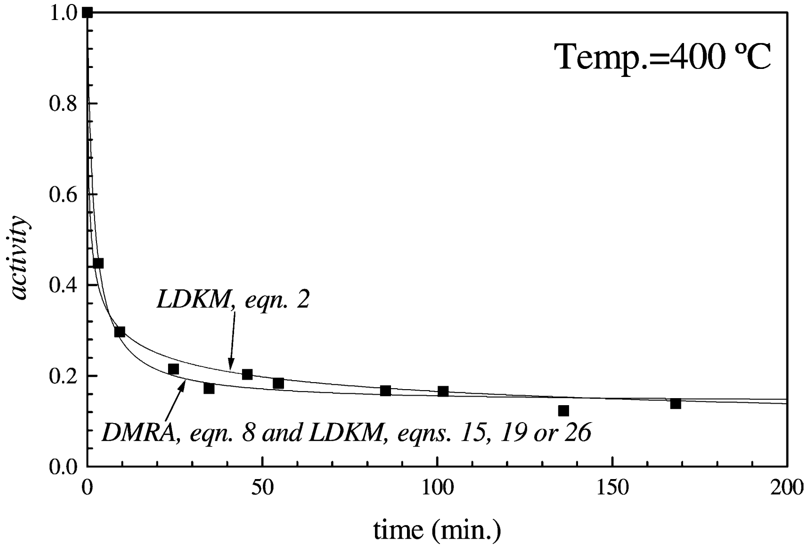

Fig. 3. Fit of the experimental data at 400 °C, obtained from Jossens and Petersen [31]. Comparison of different deactivation kinetic models.

behavior and sometimes this fact has been wrongly considered as a variation of the *deactivation order* [27–29].

In this case the evolution of the *deactivation order* is directly obtained substituting Eqs. (7) and (8) in Eq. (23).

$$d(t) = 1 - \frac{a}{(a')t} = 1 + \left(a_{S_2} + \frac{(1-a_{S_2})}{1+(1-a_{S_2})\psi^*_{d_2}t}\right) \times \left[\psi^*_{d_2}t\left(\frac{1-a_{S_2}}{1+(1-a_{S_2})\psi^*_{d_2}t}\right)^2\right]^{-1} \qquad (24)$$

In addition, the evolution of the *deactivation function* can be deduced substituting Eqs. (7), (8) and (24) in Eq. (17).

$$\psi_d(t) = \psi^*_{d_2}\left(\frac{1-a_{S_2}}{1+(1-a_{S_2})\psi^*_{d_2}t}\right)^2 \times \left(a_{S_2} + \frac{1-a_{S_2}}{1+(1-a_{S_2})\psi^*_{d_2}t}\right)^{-d(t)} \qquad (25)$$

The above equation is similar to Eq. (18), but now the *deactivation order* appearing in the exponent of the denominator, is not a constant but varies over time in accordance with Eq. (24).

Finally, for this case the activity can be calculated solving the following differential equation taking Eqs. (24) and (25) into consideration

$$\frac{\mathrm{d}a}{\mathrm{d}t} = -\psi_d(t)a^{d(t)} \qquad (26)$$

Again, the activity values predicted by Eqs. (26) and (8) are equal, as is shown in Figs. 1–3.

Eqs. (14), (18), (24) and (25) show how the variations of the kinetic parameters of the *LKDM* do not in fact have any physical meaning, but are only a consequence of a mathematical artifact due to the use of an inadequate kinetic model. On the contrary, when appropriate models, such as *DMRA* are used, the kinetic parameters do not vary as a function of time and have realistic values from a physical point of view.

3. Application to experimental data

The equations presented above have been applied to study the deactivation data obtained by Jossens and Petersen in the dehydrogenation of methyl cyclohexane, using Pt/Al_2O_3 and Pt-Re/Al_2O_3 reforming catalysts [31,32].

In these studies, the effect of the process variables, such as methyl cyclohexane concentration, toluene concentration, hydrogen partial pressure and the operating temperature have been investigated [31]. It is important to note that, in all the cases, the activity versus time plots displayed in references [31,32] indicate the existence of a residual activity.

For example, Fig. 6 of reference [31] shows the effect of the hydrogen partial pressure, indicating that the residual activity increased as the H_2 concentration was increased. In addition, Fig. 3 of referene [32] show the hydrogen reactivation of a Pt-Re fouled catalyst generation. Then, the existence of a residual activity could be related to the partial regeneration of the fouled sites by hydrogen, via a mechanism involving the reaction between coke precursors and H_2 [5,32,33]. Hence, the residual activity should be a function of the equilibrium constant in the deactivation–regeneration process [11,18–22].

In subsequent papers, the deactivation data obtained by Jossens and Petersen [31,32] were re-interpreted by Pacheco and Petersen [28,29]. These authors developed a complex deactivation model for catalyst fouling based on the *LDKM*. In this model, the "*Multiplet Fouling Model*" [29], the variation of the deactivation kinetic order was assumed.

These deactivation data can also be alternatively explained using a deactivation model with residual activity. Here, we

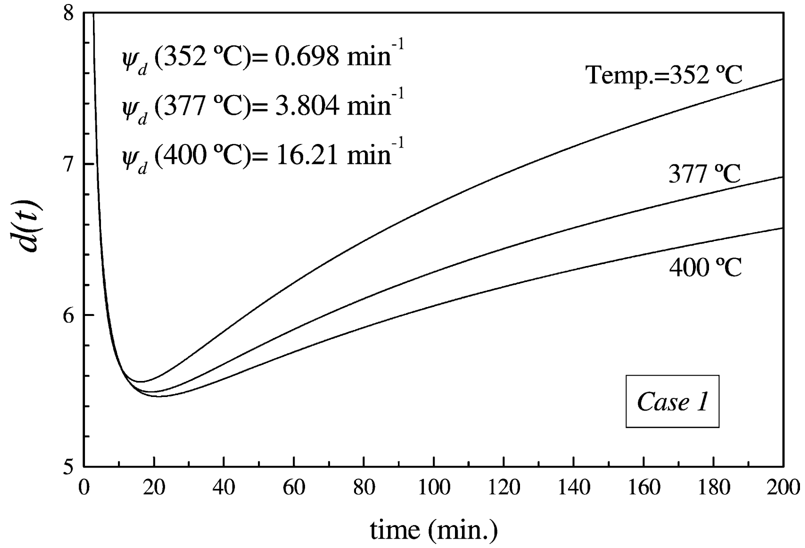

Fig. 4. Evolution of the *deactivation order* of *LDKM* according to Case 1.

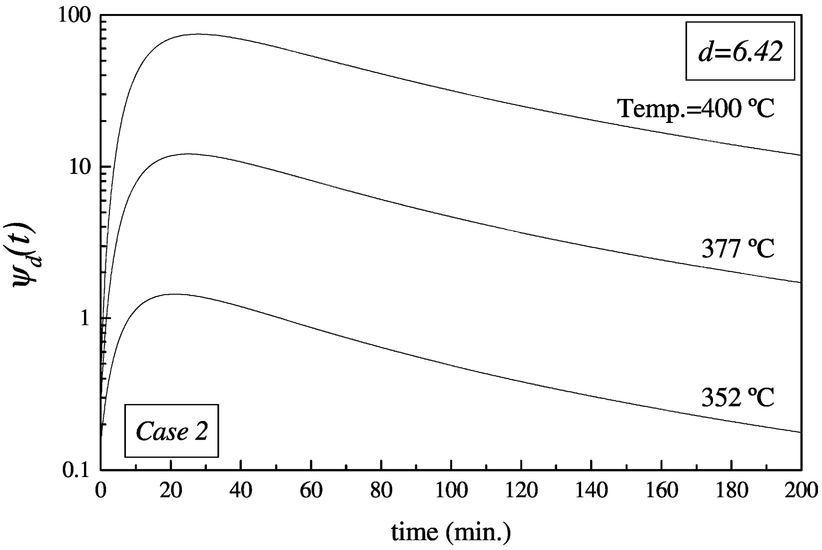

Fig. 5. Evolution of the *deactivation function* of *LDKM* according to Case 2.

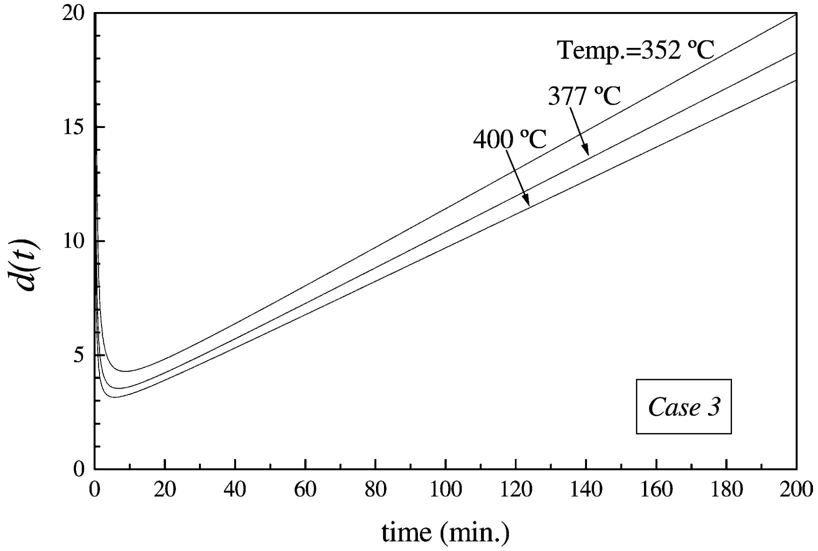

Fig. 6. Evolution of the *deactivation order* of *LDKM* according to Case 3.

use the *DMRA* model represented by Eq. (4c) to analyze the deactivation data reported in Figs. 4–7 of reference [31]. In addition, these data were also fitted using the *LDKM*. Only the effect of the reaction temperature on the deactivation behavior (see Fig. 7 of reference [31]) is reported. The best fittings were obtained when a deactivation order $d^* = 2$ for the *DMRA* model (Eq. (8)) was used.

The deactivation kinetic parameters obtained using both deactivation models, *DMRA* and *LDKM*, are summarized in Tables 1–4.

The results shown in Tables 1 and 2 correspond to the parameters obtained by non-linear regression of the activity versus time curves to the *LDKM* and *DMRA* respectively. These tables also show the values of χ^2 and R^2 as indicative of the goodness of the fittings. Given that the number of parameters is the same in both models, a direct comparison of

Table 1
Influence of the temperature on the parameters of *LDKM*

Temperature (°C)	ψ_d (min^{-1})	d	χ^2	R^2
352	3.55 ± 3.97	8.59 ± 1.37	0.0035	0.9080
377	1.19 ± 0.52	5.31 ± 0.43	0.00163	0.9626
400	2.86 ± 2.18	4.91 ± 0.65	0.00192	0.9693

Monovariable fitting.

Table 2
Influence of the temperature on the parameters of *DMRA*

Temperature (°C)	$\psi^*_{d_2}$ (min^{-1})	a_{S_2}	χ^2	R^2
352	0.341 ± 0.0484	0.291 ± 0.010	0.00084	0.97799
377	0.345 ± 0.049	0.180 ± 0.011	0.00133	0.96948
400	0.627 ± 0.0534	0.140 ± 0.006	0.00029	0.99529

Monovariable fitting.

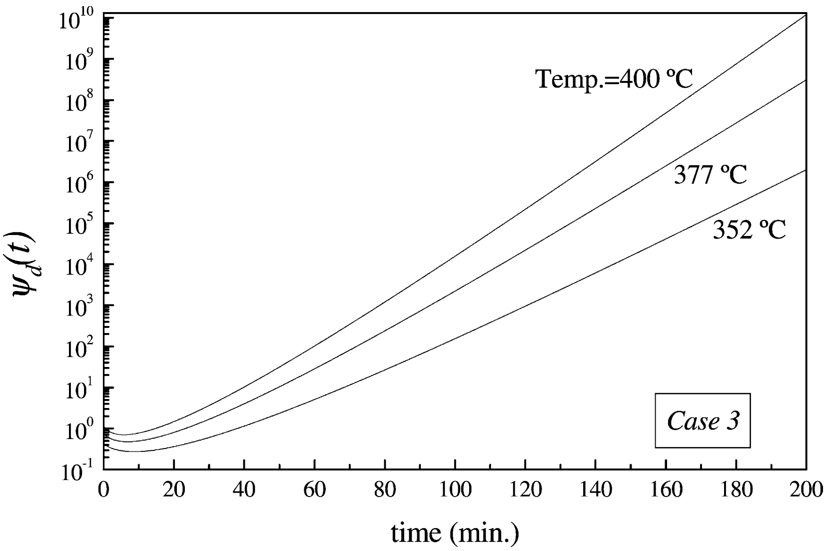

Fig. 7. Evolution of the *deactivation function* of *LDKM* according to Case 3.

Table 3
Intrinsic parameters of *LDKM*

Parameter	Value ± S.E.
χ^2	0.00266
R^2	0.9443
ψ_{d_m} (min^{-1})	0.698 ± 0.279
E_d (kJ/mol)	229.1 ± 34.2
d	6.42 ± 0.49

Multivariable fitting. Temperature of reparameterisation: 625 K.

Table 4
Intrinsic parameters of *DMRA*

Parameter	Value ± S.E.
χ^2	0.00093
R^2	0.98107
ψ^*_{d2m} (min^{-1})	0.301 ± 0.039
$E^*_{d_2}$ (kJ/mol)	44.2 ± 14.7
$A_{S_{20}}$	0.285 ± 0.011
E_{S_2} (kJ/mol)	−55.1 ± 5.8

Multivariable fitting. Temperature of reparameterisation: 625 K.

the values of χ^2 and R^2 allows the best model to be selected from a statistical point of view. The *DMRA* is shown to be a better model because it presents higher values of R^2 and lower values of the χ^2 for the three temperatures. Furthermore, and more importantly, as can be seen in Table 1, the variation with the temperature of the deactivation function of the *LDKM* does not follow a clear pattern. In addition, the deactivation order changes with the temperature and takes very high values in all the cases. It is very difficult to explain these facts from a mechanistic point of view.

On the other hand, the parameters of the *DMRA* follow a logical trend and have values within the expected range. As was anticipated, the deactivation function, ψ^*_d, increases with the temperature and the residual activity has values of between 0 and 1 in all the cases, see Table 2. Figs. 1–3 show the fitting with the different models of data obtained at the three temperatures studied by Jossens and Petersen [31].

In order to calculate the activation energies involved in the deactivation process, a non-linear multivariable regression analysis of all the curves was made with both models. In the case of the *LDKM*, we assume a constant value for the deactivation order and an Arrhenius-type dependence for the deactivation function. This dependence can be expressed in a reparameterised form as follows:

$$\psi_d = \psi_{d_0} \exp\left(-\frac{E_d}{RT}\right) = \psi_{d_m} \exp\left(-\frac{E_d}{R}\left(\frac{1}{T} - \frac{1}{T_m}\right)\right) \tag{27}$$

where:

$$\psi_{d_m} = \psi_{d_0} \exp\left(-\frac{E_d}{RT_m}\right) \tag{28}$$

In this case we select $T_m = 625$ K (352 °C). In Table 3 are shown the values of ψ_{d_m}, E_d and d and the values of χ^2 and R^2. It can be seen that the value of ψ_{d_m} ($0.698 \pm 0.279\,\mathrm{min}^{-1}$) is quite different from the value of ψ_d estimated at 352 °C ($3.55 \pm 3.97\,\mathrm{min}^{-1}$), see Table 1. These values would be quite similar if the model was adequate. The estimated value of the apparent activation energy is 54.8 kcal/mol (229.1 ± 34.2 kJ/mol). Jossens and Petersen [31] give a value of 39 kcal/mol for the period of the slow deactivation (attained at long times) and 8 kcal/mol for the initial period of rapid deactivation. For the same reaction of dehydrogenation of methyl cyclohexane and using a Pt-Re/Al_2O_3 catalyst, Pal et al. [34] calculate a value of 35 kcal/mol for the activation energy of deactivation, using the *LDKM* with $d = 2$. Pacheco and Petersen [28], using the *LDKM*, obtained a value of 74 kcal/mol. In this study, these authors are implicitly using a value $d = 6$. As can be seen in Table 3, the calculations of these authors are in very good agreement with the values obtained in the present work using the *LDKM*.

In the case of the *DMRA*, we assume Arrhenius-type dependence for both parameters. For the deactivation function, $\psi^*_{d_2}$, the equation is

$$\psi^*_{d_2} = \psi^*_{d20} \exp\left(-\frac{E^*_{d_2}}{RT}\right) = \psi^*_{d2m} \exp\left(-\frac{E^*_{d_2}}{R}\left(\frac{1}{T} - \frac{1}{T_m}\right)\right) \quad (29)$$

where

$$\psi^*_{d2m} = \psi^*_{d20} \exp\left(-\frac{E^*_{d_2}}{RT_m}\right) \quad (30)$$

For the residual activity, we can get

$$a_{S_2} = A_{S20} \exp\left(-\frac{E_{S_2}}{RT}\right) = A_{S2m} \exp\left(-\frac{E_{S_2}}{R}\left(\frac{1}{T} - \frac{1}{T_m}\right)\right) \quad (31)$$

where

$$a_{S2m} = A_{S20} \exp\left(-\frac{E_{S_2}}{RT_m}\right) \quad (32)$$

The results of this fitting are shown in Table 4. Again, a comparison of the values of χ^2 and R^2 in Table 4 with those of Table 3 indicates that the *DMRA* is the best model, even taking into account that it has one more parameter.

In Table 2, it can be seen that the values of ψ^*_{d2m} ($0.301 \pm 0.039\,\text{min}^{-1}$) and of A_{S20} (0.285 ± 0.011) are quite similar to the values of $\psi^*_{d_2}$ and a_{S_2} estimated at 352 °C ($0.341 \pm 0.0484\,\text{min}^{-1}$ and 0.291 ± 0.010, respectively). This fact indicates the reliability of this model. The estimated value of the $E^*_{d_2}$ is 10.6 kcal/mol (44.2 ± 14.7 kJ/mol), this value being five times lower than the activation energy calculated with the *LDKM*, Table 3. Bartholomew [26] found that frequently, the activation energies predicted by the *DMRA* are between 2 and 10 times lower than those predicted by the *LDKM*, and this fact is a consequence of over-estimation of the deactivation function obtained when the *LDKM* is used.

As has already been mentioned, the presence of the residual activity could be explained regarding the deactivation process as reversible. Thus, it is considered that the coke formation occurs through a reversible scheme, as already was suggested by Wolf and Petersen, [5,33].

$$P(\text{coke precursor}) + hl(h\ \text{active sites}) \Leftrightarrow Pl_h \downarrow (\text{coke}) + \text{H}_2$$

According to this, a fraction of the fouled sites can be regenerated by means of the reaction of coke with hydrogen. Therefore, the concentration of coke at the equilibrium would be determined by the operating conditions. This would explain why increase the hydrogen concentration in the feed increases the residual activity, [31] given that the coke concentration at the equilibrium diminishes.

Furthermore, it is also observed that an increase in the operating temperature reduces the residual activity, Figs. 1–3. This suggests that the activation energy of the coke formation stage is greater than that of the reactivation of the fouled sited with hydrogen. The negative value of the parameter E_{S_2} can then be explained considering that the value of the residual activity depends on the ratio between the rate of coke formation and the reverse reaction. In fact, this apparent negative activation energy would be the difference between the activation energies of both stages [22].

Furthermore, using Eqs. 14 (Case 1), 18 (Case 2) and 24 and 25 (Case 3), allows us to calculate the evolution over time of the values of the kinetic parameters involved in the *LDKM*. In these equations the values of $\psi^*_{d_2}$ and a_{S_2} are calculated from the values shown in Table 4. In addition, the values of ψ_d in Eq. (14), and d in Eq. (18), are calculated from the values presented in Table 3. The choice of these values is one of the aspects to be considered when using either of the two first cases. In principle, any value would be valid but the simplest and most logical choices would be using the values of ψ_d and d shown in Table 1 or the values calculated from the parameters shown in Table 3. On the other hand, for Case 3 it is not necessary to take any initial value for the parameters.

Figs. 4–7 is shown the evolution of d and ψ_d for the three cases studied. In Figs. 4 (Case 1) and 6 (Case 3) it can be seen that the *deactivation kinetic order* tends towards infinitum as the time tends to zero, for the three temperatures studied. At short times, the value of d diminishes dramatically until reaching a minimum value. From this point on the deactivation order increases continuously over time. However in Case 3, for times above the minimum, i.e. the application range of Case 3, $((d - 1)\psi_d t \gg 1)$, the increase of d is nearly linear and the values of d are higher than those calculated for Case 1. Moreover, in both cases the values of d are almost identical at all temperatures until the minimum is reached, after which they are different for each temperature. After the minimum, the deactivation order decreases as the temperature increases. This trend is similar to that observed for the values of d in Table 1. Fig. 6 also provides an explanation of why in various studies of deactivation by sintering, very high values of d (up to 15) have been obtained using the $\log(a)$ versus $\log(t)$ plot [35,36].

Fig. 5 shows the evolution of ψ_d predicted in Case 2. It can be seen how, in this case, the value of ψ_d evolves over time in the opposite way to the deactivation order predicted in Cases 1 and 3. Thus, at short times it increases sharply until reaching a maximum value from which point it diminishes continuously with time. Fig. 7 presents the values of ψ_d calculated according to Case 3. In this case, ψ_d increase dramatically along the time, attaining values of 10^{10}. Contrary to Case 2, where d is considered constant, in Case 3 the value of d increases continuously over time, resulting in a lower value of the denominator in Eq. (25) and therefore an increase of the values of ψ_d. Finally, as expected, at any given time the temperature increase raises the value of ψ_d.

4. Conclusions

It has been shown that the parameters of the *LDKM* must vary continuously over time when this model is used to fit deactivation data with residual activity. This fact could lead to systematic errors in estimating intrinsic parameters, such as activation energies or pre-exponential factors.

The variation of the *deactivation order* and the *deactivation function* over time cannot normally be related to a physical phenomenon, e.g. a change in the reaction mechanism, instead is only the consequence of a mathematical artifact.

The three cases developed here allow the establishment of a mathematical relationship between the deactivation parameters of two different kinetic models, *LDKM* and *DMRA*. The most suitable kinetic model for a given set of experimental data can be determined, avoiding misleading conclusions about the mechanism involved in the reaction under consideration.

The methodology developed in this work allows the correlation of the kinetic parameters of different deactivation kinetic models and their evolution as a function of time and provides a valuable tool for comparing and discriminating between different models used in kinetic studies. This does not involve new methods for fitting kinetic data, but rather to emphasize the importance of using appropriate models to reach conclusions with a real physical meaning.

Acknowledgements

The authors acknowledge financial support from DGI-MCYT, Madrid, Spain (Grant PPQ2001-2479).

References

[1] S. Krishnaswamy, J.R. Kittrell, Deactivation disguised kinetics, Ind. Eng. Chem. Process Des. Dev. 17 (1978) 200–204.

[2] S. Szépe, O. Levenspiel, Catalyst deactivation, in: Proceedings of the fourth European Symposium on Chemical Reactive Engeneering, Pergamon Press, Brussels, NY, 1971, pp. 265–276.

[3] O. Levenspiel, Experimental search of a simple rate equation to describe deactivating porous catalyst particles, J. Catal. 25 (1972) 265–272.

[4] C. Chu, Effect of adsorption on the fouling of catalysts pellets, Ind. Eng. Chem. Fundam. 7 (1968) 509–514.

[5] E.E. Wolf, E.E. Petersen, On the kinetics of self-poisoning catalytic reactions, J. Catal. 47 (1977) 28–32.

[6] J. Corella, J.M. Asua, J. Bilbao, Kinetics of catalyst deactivation, Canad. J. Chem. Eng. 59 (1981) 647–648.

[7] J. Corella, J.M. Asua, Kinetic equations of mechanistic type with non-separable variables for catalyst deactivation by coke. Models and data analysis methods, Ind. Eng. Chem. Proc. Des. Dev. 21 (1982) 55–61.

[8] R.D. Srivastava, A.K. Guha, Kinetics and mechanism of deactivation of Pd-Al_2O_3 catalyst in the gaseous phase decarbonilation of furfural, J. Catal. 91 (1985) 254–262.

[9] J. Corella, A. Monzón, J.B. Butt, R.P.L. Absil, The modelling of the kinetics of deactivation a commercial hydrocracking catalysts in the reaction of cumene disproportionation, J. Catal. 100 (1986) 149–157.

[10] G.A. Fuentes, Catalyst deactivation and steady-state activity: a generalised power-law equation model, Appl. Catal. 15 (1985) 33–40.

[11] J. Corella, J. Adanez, A. Monzón, Some intrinsic kinetic equations and deactivation mechanisms leading to deactivation curves with residual activity, Ind. Eng. Chem. Res. 27 (1988) 375–381.

[12] A. Borgna, T.F. Garetto, A. Monzón, Modelling of sulphur deactivation of naphtha-reforming catalysts. Structure sensitivity in cyclopentane hydrogenolisis, J. Chem. Soc., Faraday Trans. 93 (1997) 2445–2450.

[13] A.L. Pozzi, H.F. Rase, Catalyst fouling, Ind. Eng. Chem. 50 (1958) 1075–1080.

[14] M. Carbucicchio, P. Forzatti, F. Trifiro, E. Tronconi, P.L. Villa, Deactivation of silica supported Fe_2O_3-MoO_3 catalyst for the oxidation of methanol, Stud. Surf. Sci. Catal. 6 (1980) 103–113.

[15] J.R. Kittrell, P.S. Tam, J.W. Eldridge, Predict poisoning rate, Hydroc. Process 64 (8) (1985) 63–67.

[16] R. Christoph, M. Baerns, Desactivierung eines nickel-trager-katalysators fur die hydrierung von restkohlenmonoxid in wasserstoff zu methan, Chem. Ing. Tech. 57 (1985) 775–778.

[17] L.R. Radovic, M.A. Vannice, Sulfur tolerance of methanol synthesis catalyst: modeling of catalyst deactivation, Appl. Catal. 29 (1987) 1–20.

[18] J.C. Rodriguez, J.A. Peña, A. Monzón, R. Hughes, K. Li, Kinetic modelling of the deactivation of a commercial silica-alumina catalyst during isopropylbencene cracking, Chem. Eng. J. 58 (1995) 7–13.

[19] A. Borgna, T.F. Garetto, A. Monzón, C.R. Apesteguía, Deactivation model with residual activity to study thioresistance and thiotolerance of naphtha-reforming catalysts, J. Catal. 146 (1994) 69–81.

[20] A. Borgna, S. Magni, J. Sepúlveda, C. Apesteguía, Selective acid–base poisoning on bifunctional alkylation reaction, Stud. Surf. Sci. Catal. 139 (2001) 213–220.

[21] E.L. Agorreta, J.A. Peña, J. Santamaría, A. Monzón, A kinetic model for activation–deactivation processes in solid catalysts, Ind. Eng. Chem. Res. 30 (1991) 111–122.

[22] T.F. Garetto, A. Borgna, A. Monzón, C. R. Apesteguía, A general kinetic model to study the redispersion and sintering of Pt/Al_2O_3-Cl naphtha reforming catalysts, in: Proceedings of the Europacat II, Maastricht, The Netherlands, 3–8 September 1995.

[23] T.F. Garetto, A. Borgna, A. Monzón, Modelling of sintering kinetics of naphtha-reforming Pt/Al_2O_3-Cl catalysts, J. Chem. Soc., Faraday Trans. 92 (1996) 2637–2640.

[24] G.A. Fuentes, E.D. Gamas, Towards a better understanding of sintering phenomena in catalysis, Stud. Surf. Sci. Catal. 68 (1991) 637–644.

[25] G.A. Fuentes, Sintering of supported metals: an overview of kinetics and mechanism, in: Proceedings of the XV Simposio Iberoamericano de Catalisis, vol. 1, Córdoba, Argentina, TI, 16–20 September, 105–114, 1996.

[26] C.H. Bartholomew, Sintering kinetics of supported metals: new perspectives from a unifying GPLE treatment, Appl. Catal. 107 (1993) 1–57.

[27] J. Corella, R. Bilbao, J.A. Molina, A. Artigas, Variation with time of the mechanism, observable order an activation energy of the catalyst deactivation by coke in the FCC process, Ind. Eng. Chem. Process Des. Dev. 24 (1985) 625–636.

[28] M.A. Pacheco, E.E. Petersen, On a general correlation for catalyst fouling, J. Catal. 86 (1984) 75–83.

[29] M.A. Pacheco, E.E. Petersen, On the development of a catalyst fouling model, J. Catal. 88 (1984) 400–408.

[30] S. Fuentes, F. Figueras, Kinetics of self-poisoning of Pd/Al_2O_3 catalysts in the hydrogenolysis of cyclopentane: influence of the dispersion of palladium and sulfate poisoning, J. Catal. 54 (1978) 397–404.

[31] L.W. Jossens, E.E. Petersen, Fouling of a platinum reforming catalysts accompanying the dehydrogenation of methyl cyclohexane, J. Catal. 73 (1982) 377–386.

[32] L.W. Jossens, E.E. Petersen, Fouling of a platinum-rhenium reforming catalysts using model reforming reactions, J. Catal. 76 (1982) 265–273.

[33] E.E. Wolf, E.E. Petersen, Kinetics of deactivation of a reforming catalyst during methylcyclohexane dehydrogenation in a diffusion reactor, J. Catal. 46 (1977) 190–203.

[34] A.K. Pal, M. Bhowmick, R. Srivastava, Deactivation kinetics of platinum-rhenium reforming catalyst accompanying the dedydrogenation of methylcyclohexane, Ind. Eng. Chem. Process Des. Dev. 25 (1986) 236–241.

[35] S.E. Wanke, P.C. Flynn, The sintering of supported metal catalysts, Catal. Rev. Sci. Eng. 12 (1975) 93–135.

[36] H.K. Kuo, P. Ganesan, R.J. De Angelis, The sintering of silica-supported nickel catalyst, J. Catal. 64 (1980) 303–319.